Histochemical analysis of osteoclast and osteoblast distributions on hydroxyapatite/collagen bone-like nanocomposite embedded in rat tibiae

Mako Sakakibara[1, 2], Tomoka Hasegawa[1#], Mai Haraguchi-Kitakamae[1], Yan Shi[1], Weisong Li[1], Jiaxin Cui[1], Xuanyu Liu[1], Tomomaya Yamamoto[1,3], Hiromi Hongo[1], Norio Amizuka[1], Yoshiaki Sato[2], and Masanori Kikuchi[4#]

[1]Ultrastructure of Hard Tissues, [2]Orthodontics, Faculty of Dental Medicine, Hokkaido University, Sapporo, Japan, [3]Department of Dentistry, Japan Ground Self-Defense Force Camp, Shinmachi, Japan, [4]Bioceramics Group, Research Center for Macromoleclules and Biomaterials, National Institute for Materials Science, Tsukuba, Japan

Running title: ***Bone substitution using hydroxyapatite and collagen***

[#]Corresponding Authors

Tomoka Hasegawa, DDS, Ph.D.
Ultrastructure of Hard Tissues,
Graduate School of Dental Medicine, Hokkaido University, Sapporo, Japan
Phone/Fax: +81-11-706-4226, E-mail: hasegawa@den.hokudai.ac.jp

Masanori Kikuchi, Ph.D.
Bioceramics Group, Research Center for Macromolecules and Biomaterials, National Institute for Materials Science, Tsukuba, Japan
Phone/Fax: +81-29-860-4503, e-mail: KIKUCHI.Masanori@nims.go.jp

Abstract

Objectives: Hydroxyapatite (HAp)/collagen (Col) cylinders with laminated collagen layers were implanted into the tibial diaphysis of rats and examined histochemically to clarify how the orientation of HAp and Col bone-like nanocomposite fibers in HAp/Col blocks affects bone resorption and formation.

Methods: HAp/Col fibers were synthesized and compressed into cylindrical blocks to mimic bone nanostructures. These were implanted into the cortical bone cavities of 10-week-old male Wistar rats with fiber bundles parallel to the tibial surface. The implants were histologically analyzed at 3, 5, 7, 14, and 28 days after implantation.

Results: TRAP-positive osteoclasts appeared after 3–5 days in the lateral region of the graft, where the fiber ends were exposed, but not in the bottom region, where the HAp/Col fibers were parallel to the surface. Osteoclasts were observed in both regions by day 14. PHOSPHO1-positive osteoblasts were first detected on day 5, appearing slightly away from the cylinder laterally but directly on the bottom surface. A few osteoblasts contacted the block laterally, whereas many were observed on the new bone tissue at the bottom, between days 7 and 14. Bone formation was induced earlier in the bottom region, whereas lateral resorption was dominant. This suggested the uncoupling of bone resorption and formation in the early postimplantation stages. However, bone remodeling shifted to coupling between osteoclasts and osteoblasts throughout the cylinder by day 28.

Conclusion: The orientation of HAp/Col fibers in HAp/Col graft materials substantially affected the preferential induction of bone resorption or formation during the early stages of bone regeneration.

Key words: HAp/Col, bone regeneration, osteoblast, osteoclast, histochemistry

1. Introduction

Calcium phosphate-based materials have long been used as bone substitute materials for grafts. Bone substitutes containing collagen fibers in addition to calcium phosphate have been developed to more closely mimic the properties of the bone matrix *in vivo*. However, the characteristics of the calcium phosphate components have been seen as the primary factors influencing the success of bone regeneration following grafting, while collagen fibers have been considered auxiliary, contributing mainly to cell adhesion and migration.

In vivo, the bone matrix consists of a 1:1 hydroxyapatite (HAp) to collagen (Col) volume ratio, corresponding to an approximate 73:27 mass ratio, which suggests that collagen fibers play a significant role in bone formation and regeneration. The collagen fiber arrangement differs significantly between mature cortical bone and immature bone tissues, such as primary trabeculae [1]. Therefore, it is crucial to consider the geometric arrangement of collagen fibers when evaluating bone regeneration using calcium phosphate-based bone grafts containing collagen fibers.

The degree of mineralization of collagen fibers in the bone matrix may depend on the individual age and the position of bone in the body. Immature bone, such as the primary trabeculae beneath the growth plate cartilage during development and growth, exhibits a histologically immature structure with randomly dispersed collagen fibrils [1], lacking a lamellar bone structure. In contrast, cortical bone, which forms the thick outer wall of long bones, exhibits a lamellar structure with bundles of collagen fibers regularly arranged in the lamellar layers [2]. In addition, the *c*-axes of HAp nanocrystals align along the long-axes of collagen molecules, forming the mineral surface of bone, *i.e.*, the *m*-surface (This is often called the *a*-surface, but the crystallographically correct name is *m*-surface; therefore, in this paper, the authors use "*m*-surface") [3]. Nakano et al. [4] also demonstrated this arrangement using X-ray diffraction analysis. Moreover, Hasegawa et al. [5] revealed that HAp crystals, which are needle-like in shape and similar in length to the periodic banding of collagen fibers, are consistently and precisely aligned along the collagen fibers. Thus, HAp crystal arrangement, along with collagen fiber arrangement, may also affect bone formation and regeneration.

In cortical bone, collagen bundles form layered structures with parallel fibers, creating a plywood-like arrangement of stacked lamellae [2]. The HAp/Col bone substitute developed by Kikuchi et al. [6] closely mimics this structure, although the collagen fibers are not unidirectional in two dimensions within each layer. This differs from other calcium phosphate-based bone substitutes with collagen fibrils, such as Bio-Oss® (Geistlich Pharma AG, Switzerland), Collagraft® (Zimmer Biomet), and BONEJECT® (GC Corporation), which have different compositions and structures [7,8]. Additionally, the HAp/Col composite can be fabricated in dense, porous, and sheet-like forms [6,9,10].

Therefore, it is possible to laminate layers of HAp/Col to form a HAp/Col cylinder with a laminate structure consisting of horizontally aligned collagen fibers in stacked sheets.

In this study, by embedding layered HAp/Col cylinders with aligned collagen fiber bundles into the cortical bone of rat tibiae, we examine whether collagen fiber orientation influences the distribution of osteoclasts and osteoblasts in regions where the fibers run perpendicular or parallel to the bone structure and assess new bone formation during bone regeneration.

2. Materials and Methods

2.1. Preparation of the HAp/Col block for bone substitute

Water for Injection (Otuska Pharmaceutical, Japan) was used in HAp/Col synthesis to avoid contamination of endotoxins. The HAp/Col bone-like nanocomposite fibers were synthesized via the previously reported simultaneous titration method [6]. Briefly, 199.1 mmol of $Ca(OH)_2$ (prepared by hydrating CaO obtained from the heat decomposition of alkaline analysis grade $CaCO_3$ [Fuji Film Wako Pure Chemical, Ind]) dispersed in 2 dm^3 of H_2O and a 59.7 mM H_3PO_4 (Fuji Film Wako Pure Chemical, Ind., Japan) aqueous solution containing 5 g of atelocollagen (derived from porcine dermis, Nitta Gelatin, Inc., Japan) were simultaneously and gradually added through respective tube pumps into a central reaction vessel containing 1 dm^3 of H_2O. The starting materials were prepared so that the final composite would have a HAp:collagen mass ratio of 80:20. A 40°C water bath controlled the reaction temperature, and the reaction solution pH was maintained at 9.0 ± 0.1 by an automatic titration unit. The precipitates were filtrated with suction and washed 3 times with H_2O.

To maintain a lamellar fiber structure, a HAp/Col disk was prepared by packing 32.6 g of the HAp/Col fibrous precipitate into a specially designed mold allowing excess water removal and uniaxially compressing it at 20 MPa for 24 h, forming a 35 mm-diameter, 3.64 mm-thick disk. Three-millimeter-diameter HAp/Col cylinders were punched out of the disk with a 3 mm punch for leather, dried in a vacuum, and sterilized with ethylene oxide gas.

2.2. Animals and the preparation of bone defects and grafts

The HAp/Col cylinders were implanted into the anterior region of the tibia of rats (Fig. 1). Thirty 10-week-old male Wistar rats (Japan SLC Co. Inc., Japan) were handled according to Hokkaido University's guidelines for animal care and research use (approved study protocol #23-0095). The rats were anesthetized with a mixture of 0.3 mg/kg of medetomidine, 4.0 mg/kg of midazolam, and 5.0 mg/kg of butorphanol. After partially shaving the right tibial region, a round cavity defect 1.5‑2.0 mm in diameter was created in the arterial center of the tibia. The site was irrigated with sterilized

physiological saline during drilling to prevent overheating. With the defect completed, an HAp/Col cylinder was placed into the defect such that the top and bottom planes of the cylinder and the collagen fiber layers were parallel to the periosteal surface of the tibia (Fig. 1). The defects were covered with the tibial skin and an instant adhesive (Aron Alpha®, TOAGOSEI, Co. Ltd., Japan).

2.3. Specimen preparation

At 3, 5, 7, 14, and 28 days after the HAp/Col grafting ($N = 6$ for each), the rats were anesthetized and perfused with 4% paraformaldehyde diluted in 0.1 M phosphate buffer (pH 7.4) through the left cardiac ventricle, and the tibiae were extracted and immediately immersed in the same solution for 24 h at 4°C. Micro-CT images were taken, and the specimens were decalcified with 10% EDTA-2Na for 2 months. The decalcified specimens were dehydrated in a series of ethanol solutions with increasing concentrations, soaked in xylene, and finally embedded in paraffin. Then, 5 μm-thick sagittal paraffin sections were cut to examine two regions of the HAp/Col cylinder: the lateral region facing the cortical bone (perpendicular to the HAp/Col layers), and the bottom region near the marrow (parallel to the collagen layers) as previously described [11,12].

2.4. Micro-CT analysis

Micro-CT images were obtained from the grafted areas using a micro-CT scanner (tube voltage 90 kV, CosmoScan FX, Rigaku Corporation, Japan) following the methods in Morimoto et al. [12]. The CT analyzer software CosmoScan Viewer (Rigaku Corporation) was employed for image reconstruction per the guidelines described by Bouxsein et al. [13].

2.5. Histochemistry for PHOSPHO1 and tartrate-resistant acid phosphatase

After inhibition of endogenous peroxidase activity with methanol containing 0.3% hydrogen peroxidase for 30 min, dewaxed paraffin sections were pretreated with 1% bovine serum albumin (BSA; Serologicals Proteins Inc., Kankakee, IL) in PBS (1% BSA-PBS) for 30 min. The sections were then incubated with rabbit polyclonal anti-PHOSPHO1 antibody (phosphoethanolamine/phosphocholine phosphatase 1; Q8TCT1, Cusabio Technology Llc., TX) diluted at 1:100 in 1% BSA-PBS at room temperature (RT) for 2 h and then incubated with horseradish peroxidase (HRP)-conjugated goat anti-rabbit IgG antibody (P0399, DakoCytomation, Denmark) at a dilution of 1:100 for 1 h at RT. Detection of tartrate-resistant acid phosphatase (TRAP) was conducted as previously described [14].

2.6. Regions of interest and TRAP-positive osteoclast and PHOSPHO1-reactive osteoblast

enumeration

Two 300 × 900 μm rectangular regions of interest (ROIs), one located in the center of the distal side of the HAp/Col cylinder and the other in the center of the bottom (marrow) side, were placed in images of the sagittal sections of tibiae to represent regions where the collagen layers of the cylinder run perpendicular and parallel to the bone structure, respectively (Fig. 1).

The total numbers of TRAP-positive osteoclasts and PHOSPHO1-reactive osteoblasts attached to the HAp/Col surface and newly formed bone in each ROI were counted as described recently in Haraguchi-Kitakamae et al. [15].

2.7. Statistical analysis

All values are expressed as means ± standard errors. Student's *t*-tests were used for two-group comparisons, and one-way ANOVAs followed by Dunnett's tests were used for multiple comparisons. *P*-values < 0.05 were considered to infer statistical significance.

3. Results

3.1. Micro-CT imaging

Micro-CT images from day 3 to 28 post-grafting showed the HAp/Col cylinder's upper surfaces parallel to surrounding cortical bone (Fig. 2). A semi-transparent tissue formed around the cylinders by day 5 (Fig. 2B), thickening into new bone by day 7 (Fig. 2C). By day 14, radiopaque trabecular bone was visible around the cylinder, the surface of which had begun to disintegrate (Fig. 2D). On day 28, the cylinder appeared osseointegrated with adjacent cortical bone, while the bottom regions of the HAp/Col cylinder showed resorption (Fig. 2E).

3.2. Chronological observations of bone development after HAp/Col cylinder grafting

On day 3 post-implantation, the HAp/Col cylinders showed a smooth surface surrounded by bone marrow tissue (Fig. 3A). The lateral region exhibited a small amount of cellular invasion into the cylinder (Fig. 3A and B). By day 5, fine trabecular bone had formed around the cylinder, with a thick cell layer on the lateral surface. Immature trabeculae were observed at a distance from the lateral surface, while the bottom surface showed continuous trabecular network extension (Fig. 3D–F). On day 7, the cylinder had become encompassed by newly formed bone with a typical trabecular structure. In the lateral region, trabeculae formation remained at a distance from the cylinder, separated by fibrous stromal tissue. The bottom surface was covered with a thin bone matrix layer, from which

trabeculae extended outward (Fig. 3G–I). On day 14, the cylinder surface appeared irregular and uneven. The lateral region lacked continuity between the new bone and the cylinder, with numerous multinucleated giant cells on the surface. Rows of cells had invaded the cylinder's interior in a parallel arrangement. The bottom region showed fragmentation into islands, with new bone filling the spaces between them (Fig. 3J–L). By day 28, the shape of the HAp/Col cylinder had collapsed, with new bone penetrating its interior. The lateral region showed integration between the HAp/Col matrix and new bone tissues, while the bottom region exhibited active bone resorption with accumulated multinucleated giant cells (Fig. 3M–O).

3.3. Chronological observations of the TRAP-positive osteoclast distributions

On day 3, numerous TRAP-positive osteoclasts were observed around the HAp/Col cylinder, with fewer at the bottom region than at the lateral (Fig. 4A–C). By day 5, osteoclasts had become more localized on the lateral surface, with fewer at the bottom (Fig. 4D–F). On day 7, many osteoclasts were found on the lateral surface, and some had invaded the cylinder's interior, while the bottom region still had fewer osteoclasts (Fig. 4G–I). By day 14, a significant number of TRAP-positive osteoclasts were present on the cylinder’s lateral surface and the surfaces of nearby newly formed bone tissue, while the bottom region showed osteoclasts on new trabeculae (Fig. 4J–L). By day 28, osteoclasts had fully invaded the cylinder, indicating strong resorption activity, on both lateral and bottom surfaces (Fig. 4M–O).

3.4. Numbers of TRAP-positive osteoclasts

We analyzed the numbers of osteoclasts attached to the HAp/Col material and newly formed bone, as well as the total number of osteoclasts in the ROIs (Fig. 5). On day 3, few TRAP-positive osteoclasts were observed around the cylinder, with no regional differences. From days 5 to 14, osteoclast numbers increased significantly, especially in the lateral region where collagen fibers intersect. The bottom region also saw an increase, but it was less pronounced. By day 28, osteoclast numbers attached to the cylinder and new bone had decreased in the lateral region to levels similar to those of the bottom region. However, the total osteoclast count remained higher in the lateral region. Taken together, these findings suggest that osteoclasts predominantly accumulate in the lateral region of the graft, where collagen fibers intersect, rather than in the bottom region, where fibers run parallel.

3.5. Chronological observations of the PHOSPHO1-positive osteoblast distributions

PHOSPHO1 is an enzyme that hydrolyzes phosphocholine and phosphoethanolamine to release phosphate ions within matrix vesicles derived from osteoblasts and chondrocytes [16, 17]. Since

chondrocytes were not found in bone regeneration sites, we employed PHOSPHO1 as a marker of bone-mineralizing osteoblasts. Three days post-surgery, no PHOSPHO1-positive osteoblasts were visible on any HAp/Col cylinder surface (Fig. 6A–C). On days 5–7, osteoblasts appeared in trabecular bone tissue around the cylinder (Fig. 6D and G). In lateral regions, they were seen in trabecular bone adjacent to the cylinder surface, but not on it (Fig. 6E and H). However, they were detected in new bone extending from the bottom surface (Fig. 6F and I). On day 14, PHOSPHO1-positive osteoblasts remained in trabecular bone distant from the lateral surface (Fig. 6J and K), while lines of them were noted on new trabecular bone in the bottom region (Fig. 6L). By day 28, rows of PHOSPHO1-positive osteoblasts extended throughout the cylinder (Fig. 6M and N) but showed a decreasing trend in the trabecular bone at the bottom region (Fig. 6O).

3.6. Numbers of PHOSPHO1-positive osteoblasts

We counted the PHOSPHO1-positive osteoblasts attached to the HAp/Col cylinder and the newly formed bone in the ROIs of the lateral and bottom regions (Fig. 7). During days 5–14, PHOSPHO1-positive osteoblasts predominantly increased in the bottom region, with significantly greater numbers counted in the bottom region than in the lateral region throughout this period. However, by the 28th day, there was no significant difference in the numbers of PHOSPHO1-positive osteoblasts between the two regions.

4. Discussion

We aimed to clarify whether the orientation of collagen fibers in a bone substitute material composed of HAp/Col fibers affects bone resorption and bone formation. To achieve this, we implanted an HAp/Col graft composed of layered collagen plates into the diaphysis of rat tibiae and conducted histological analyses. Our findings revealed distinct patterns of osteoclast and osteoblast localization in different regions of the implant during the early post-implantation period (5–14 days). In the lateral region, where collagen fiber ends were exposed, numerous osteoclasts accumulated on the HAp/Col cylinder surface and resorbed them, with minimal osteoblasts present. Therefore, bone remodeling may occur in the lateral region. Conversely, the bottom region, where collagen fibers ran parallel, exhibited predominantly osteoblastic bone formation, with lower osteoclast accumulation, suggesting bone modeling (Fig. 8). These findings suggest that the orientation of collagen fibers influences the early localization of osteoclasts and osteoblasts, uncoupling osteoclastic bone resorption and osteoblastic bone formation, which affects bone modeling and has significant implications for bone regeneration.

Hydroxyapatite and beta-tricalcium phosphates are well-known osteoconductive materials that serve as scaffolds for bone cell migration and attachment [18–23]. Previous research indicates that bone substitute material replacement is similar to bone remodeling, with osteoclasts first resorbing the osteoconductive material, followed by osteoblast migration and bone matrix addition [23,24], making it distinct from bone modeling, even during bone regeneration.

To facilitate cell infiltration into calcium phosphate-based bone substitutes, various improvements have been made, including optimizing granule and pore sizes and incorporating collagen fibers [25−28]. However, the orientation of collagen fibers has received relatively little attention. Therefore, we examined how collagen fiber orientation affected bone resorption and formation. To do this, it is necessary to exclude other factors that would induce bone resorption and bone formation, for instance, mechanical stress and the osteocytic lacunar canalicular system [30−32]. We embedded the HAp/Col graft avoiding tight contact between the embedded cylinders and the surrounding bone tissue of the rat tibiae, avoiding mechanical stress. In addition, there was no living osteocytic network in the HAp/Col cylinder. Therefore, we believe that our study excluded these factors. We hypothesize that, in the absence of mechanical stress, the orientation of collagen fibers affects the localization of osteoclast and osteoblast accumulation.

One may wonder “Why did osteoclasts accumulate in the graft’s lateral region, where the fiber ends are exposed at the surface, while bone formation by osteoblasts was induced in the bottom region, where the collagen fibers run parallel to the surface?” According to the studies by Hasegawa et al. [33], osteoblast projections show two types: one that extends perpendicularly to the bone surface to connect with osteocytes and another that encompasses collagen bundles. Therefore, there is a relationship between the orientation of osteoblast projections and that of collagen fiber bundles, and the present study’s findings suggest that HAp/Col fibers running parallel to the secretion surface of osteoblasts may be more advantageous, *e.g.,* for cell adhesion via integrins [34]. On the other hand, the bone resorption compartment of osteoclasts, which is also responsible for collagen reabsorption, has a characteristic ruffled border, and it seems that collagen fibers oriented perpendicularly to this resorption surface may be more easily absorbed. In addition, several researchers have mentioned that HAp crystals have different properties depending on their surface orientation. Specifically, the *m*-surface and *c*-surface of HAp exhibit differences in crystal solubility, protein adsorption, and cell growth [35,36]. Aizawa et al. [37] demonstrated that osteoblasts promoted mineralization when cultured *in vitro* on HAp ceramics with the *m*-surfaces exposed. In our study, the bottom surface of the HAp/Col cylinders, where the *m*-surfaces of the HAp crystals is exposed, induced osteoblastic bone formation. Thus, the orientation of both collagen fibers and HAp crystals may contribute to osteoblast induction.

The distinct osteoclast and osteoblast accumulation patterns associated with the different HAp/Col fiber orientations were most pronounced during the early stages of graft recovery in this study. As bone resorption and bone formation progressed, the distribution of osteoclasts and osteoblasts within the HAp/Col cylinder became indistinct over time. This is likely due simply to the nature of the bone remodeling process, which has previously been described [38,39]. Therefore, in the context of bone reconstruction, if the orientation of collagen fibers in the HAp/Col graft can be standardized to induce osteoclast or osteoblast accumulation in desired areas, it may be possible to guide bone regeneration in a controlled manner during the early stages.

One limitation of this study is that, while the HAp/Col fibers were aligned in one plane, they still pointed in various directions within that plane, meaning that the structure did not fully mimic the geometric structure of lamellar bone tissue. However, given this study's results, HAp/Col graft designs with refined collagen fiber orientations are anticipated. Additionally, while enumerating TRAP-positive osteoclasts and PHOSPHO1-positive osteoblasts, especially in the late stages, it was hard to distinguish osteoclasts and osteoblasts located on the HAp/Col surface from those on the newly formed bone. Therefore, in this study, we counted the cells located on the cylinder and the new bone together. Additionally, further analysis is required to elucidate the mechanisms by which collagen fiber and HAp crystal alignment induce distinct localizations of osteoclasts and osteoblasts.

5. Conclusions

This study's results suggest that when an HAp/Col graft with HAp/Col fibers in a planar orientation is implanted into the tibial cavity of rats, osteoclasts accumulate in the region where the collagen fiber ends are exposed, while osteoblasts tend to adhere and induce bone formation in the regions where the collagen fibers run parallel to the bone tissue's surface. In bone reconstruction, controlling the orientation of collagen fibers in HAp/Col bone substitute materials may allow for targeted bone resorption or the promotion of bone formation in specific regions, potentially enabling surgeons to guide bone regeneration in a predictable manner.

Ethical standards

All animal experiments were performed in accordance with the Japanese Act on Welfare and Management of Animals. The protocol was approved by the Institutional Animal Care and Use

Committee of Hokkaido University (approved research proposal #23-0095).

Competing interests

The authors declare no competing interests.

Contributors

Hasegawa T and Kikuchi M designed this study and prepared the final draft of the article. Sakakibara M is the first author in charge of writing the original draft and analyzing and interpreting the data. Haraguchi-Kitakamae M, Shi Y, Li W, Liu X, and Hongo H contributed to the histochemical analysis. Cui J and Yamamoto T worked on the statistical analyses and critically read the manuscript. Sato Y and Amizuka N participated in the discussion, editing, and formatting of the manuscript.

Funding Statement

This study was partially supported by grants from the Japan Society for the Promotion of Science (JSPS, 24K02609 to Amizuka N, 22K0991 to Hasegawa T, 24K12864 to Yamamoto T, 23K09115 to Hongo H) .

Reference

[1] Shapiro F, Wu JY. Woven bone overview: structural classification based on its integral role in developmental, repair and pathological bone formation throughout vertebrate groups. ***Eur Cell Mater.*** 38:137-167, 2019.

[2] Yamamoto T, Hasegawa T, Hongo H, Amizuka N. Alternating lamellar structure in human cellular cementum and rat compact bone: Its structure and formation. ***J Oral Biosci.*** 61(2):105-114, 2019.

[3] Sasaki, N. and Sudoh, Y.: X-ray pole figure analysis of apatite crystals and collagen molecules in

bone. ***Calcif Tissue Int***. 60, 361-367, 1997.

[4] Nakano T, Kaibara K, Tabata Y, Nagata N, Enomoto S, Marukawa E, et al. Unique alignment and texture of biological apatite crystallites in typical calcified tissues analyzed bymicrobeam X-ray diffractometer system. ***Bone.*** 31(4):479-87, 2002.

[5] Hasegawa T, Li M, Hara K, Sasaki M, Tabata C, Freitas PHL, et al. Morphological assessment of bone mineralization in tibial metaphyses of ascorbic acid-deficient ODS rats. ***Biomed Res.*** 32(4):259-269, 2011.

[6] Kikuchi M, Itoh S, Ichinose S, Shinomiya K, Tanaka J. Self-organization mechanism in a bone-like hydroxyapatite/collagen nanocomposite synthesized in vitro and its biological reaction in vivo. ***Biomaterials.*** 22: 1705-1711, 2001.

[7] Wang J, Cui W, Zhao Y, Lei L, Li H. Clinical and radiographic evaluation of Bio-Oss granules and Bio-Oss Collagen in the treatment of periodontal intrabony defects: a retrospective cohort study. ***J Appl Oral Sci.*** 32: e20230268, 2024.

[8] Cornell CN, Lane JM, Chapman M, Merkow R, Seligson D, Henry S, et al. Multicenter trial of Collagraft as bone graft substitute. ***J Orthop Trauma*** 5(1):1-8, 1991.

[9] Kikuchi M, Ikoma T, Syoji D, Matsumoto HN, Koyama Y, Itoh S, et al. Porous body preparation of hydroxyapatite/collagen nanocomposites for bone tissue regeneration. ***Key Eng Mater.*** 254-256:561-4, 2004.

[10] Kikuchi M. Osteogenic activity of MG63 cells on hydroxyapatite/collagen nanocomposite membrane. ***Key Eng Mater.*** 330-332: 313-6, 2007.

[11] Hasegawa T, Yamamoto T, Sakai S, Miyamoto Y, Hongo H, Qiu Z, et al. Histological Effects of the Combined Administration of Eldecalcitol and a Parathyroid Hormone in the Metaphyseal Trabeculae of Ovariectomized Rats. ***J Histochem Cytochem.*** 67(3):169-184, 2019.

[12] Morimoto Y, Hasegawa T, Hongo H, Yamamoto T, Maruoka H, Haraguchi-Kitakamae M, Nakanishi K, Yamamoto T, Ishizu H, Shimizu T, Yoshihara K, Yoshida Y, Sugaya T, Amizuka N. Phosphorylated pullulan promotes calcification during bone regeneration in the bone defects of rat tibiae. ***Front Bioeng Biotechnol.*** 11:1243951, 2023.

[13] Bouxsein ML, Boyd SK, Christiansen BA, Guldberg RE, Jepsen KJ, Muller R. Guidelines for

assessment of bone microstructure in rodents using micro-computed tomography. ***J Bone Min Res.*** 25: 1468–1486, 2010.

[14] Hasegawa T, Tokunaga S, Yamamoto T, Sakai M, Hongo H, Kawata T, et al. Evocalcet rescues secondary hyperparathyroidism-driven cortical porosity in chronic kidney disease male rats. ***Endocrinology.*** 164(4): bqad022, 2023.

[15] Haraguchi-Kitakamae M, Nakajima Y, Yamamoto T, Hongo H, Cui J, Shi Y, et al. Regional difference in the distribution of alkaline phosphatase, PHOSPHO1, and calcein labeling in the femoral metaphyseal trabeculae in parathyroid hormone-administered mice. ***J Oral Biosci.*** 66(3):554-566, 2024.

[16] Roberts SJ, Stewart AJ, Sadler PJ, Farquharson C. Human PHOSPHO1 exhibits high specific phosphoethanolamine and phosphocholine phosphatase activities. ***Biochem. J.*** 82:59–65, 2004.

[17] Roberts S, Narisawa S, Harmey D, Millán J.L, Farquharson C. Functional involvement of PHOSPHO1 in matrix vesicle-mediated skeletal mineralization. ***J. Bone Miner. Res.*** 22:617–627, 2007.

[18] Block MS, Kent JN. Long-term radiographic evaluation of hydroxylapative-augmented mandibular alveolar ridges. ***J Oral Maxillofac Surg.*** 42: 793–796, 1984.

[19] Bifano CA, Edgin WA, Colleton C, Bifano SL, Constantinoet PD. Preliminary evaluation of hydroxyapatite cement as an augmentation device in the edentulous atrophic canine mandible. ***Oral Surg Oral Med Oral Pathol Oral Radiol Endod.*** 85: 512–516, 1998.

[20] Liljensten E, Adolfsson E, Strid KG, Thomsen P. Resorbable and nonresorbable hydroxyapatite granules as bone graft substitutes in rabbit cortical defects. ***Clin Implant Dent Relat Res.*** 5: 95–102, 2003.

[21] Tapety FI, Amizuka N, Uoshima K, Nomura S, Maeda T. A histological evaluation of the involvement of Bio-OssR in osteoblastic differentiation and matrix synthesis. ***Clin Oral Implants Res.*** 15: 315–324, 2004.

[22] Lee YM, Shin SY, Kim JY, Kye SB, Ku Y, Rhyu IC. Bone reaction to bovine hydroxyapatite for maxillary sinus floor augmentation: histologic results in humans. ***Int J Periodontics Restor Dent.*** 26: 471–481, 2006.

[23] Nakadate M, Amizuka N, Li M, Freitas PHL, Oda K, Nomura S, et al. Histological evaluation on bone regeneration of dental implant placement sites grafted with a self-setting alpha-tricalcium phosphate cement. ***Microsc Res Tech.*** 7: 93–104, 2008.

[24] Kojima T, Amizuka N, Suzuki A, de Freitas PH, Yoshizawa M, Kudo A, et al. Histological examination of bone regeneration achieved by combining grafting with hydroxyapatite and thermoplastic bioresorbable plates. ***J Bone Min Metab.*** 25: 361–373, 2007.

[25] An J, Liao H, Kucko NW, Herber RP, Wolke JG, van den Beucken JJ, et al. Long-term evaluation of the degradation behavior of three apatite-forming calcium phosphate cements. ***J Biomed Mat Res A*** 104: 1072–1081, 2016.

[26] Chang YL, Lo YJ, Feng SW, Huang YC, Tsai HY, Lin CT, et al. Bone healing improvements using hyaluronic acid and hydroxyapatite/beta-tricalcium phosphate in combination: an animal study. ***Biomed Res Int.*** 2016: 8301624, 2016.

[27] Pilliar RM, Kandel RA, Grynpas MD, Theodoropoulos J, Hu Y, Allo B, et al. Calcium polyphosphate particulates for bone void filler applications. ***J Biomed Mater Res B Appl Biomater.*** 105: 874–884, 2017.

[28] Bohner M, Santoni BLG, Döbelin N. β-Tricalcium phosphate for bone substitution: synthesis and properties. ***Acta Biomater.*** 113: 23–41, 2020.

[29] Saito S, Hamai R, Shiwaku Y, Hasegawa T, Sakai S, Tsuchiya K, et al. Involvement of distant octacalcium phosphate scaffolds in enhancing early differentiation of osteocytes during bone regeneration. ***Acta Biomater.*** 129: 309–322, 2021.

[30] Bikle DD, Halloran BP. The response of bone to unloading. ***J Bone Miner Metab.*** 17: 233-44, 1999.

[31] Chen H, Senda T, Kubo KY. The osteocyte plays multiple roles in bone remodeling and mineral homeostasis. ***Med Mol Morphol.*** 48: 61-68, 2015.

[32] Wang L, You X, Lotinun S, Zhang L, Wu N, Zou W. Mechanical sensing protein PIEZO1 regulates bone homeostasis via osteoblast-osteoclast crosstalk. ***Nat Commun.*** 11: 282, 2020.

[33] Hasegawa T, Yamamoto T, Hongo H, Qiu Z, Abe M, Kanesaki T, et al. Three-dimensional ultrastructure of osteocytes assessed by focused ion beam-scanning electron microscopy (FIB-SEM).

Histochem Cell Biol. 149: 423-432, 2018.

[34] Jokinen J, Dadu E, Nykvist P, Käpylä J, White DJ, Ivaska J, et al. Integrin-mediated cell adhesion to type I collagen fibrils. ***J Biol Chem.*** 279: 31956-63, 2004.

[35] Chen W, Tian B, Lei Y, Ke QF, Zhu ZA, Guo YP. Hydroxyapatite coatings with oriented nanoplate and nanorod arrays: Fabrication, morphology, cytocompatibility and osteogenic differentiation. ***Mater Sci Eng C Mater Biol Appl.*** 67, 395–408, 2016.

[36] Onuma E, Honda T, Yoshimura H, Nishihara T, Ogura A, Kanzawa N, et al. Identification of Proteins Adsorbed on Hydroxyapatite Ceramics with a Preferred Orientation to a-Plane. ***Crystals***. 13, 1318, 2023.

[37] Aizawa M. Development of bioceramics with life functions by harnessing crystallographic anisotropy and their biological evaluations. ***J Ceram Soc Jpn.*** 128, 997–1004, 2020.

[38] Itoh S, Kikuchi M, Takakuda K, Nagaoka K, Koyama Y, Tanaka J, et al. Implantation study of a novel hydroxyapatite/collagen (HAp/col) composite into weight-bearing sites of dogs. ***J Biomed Mater Res.*** 63: 507-15, 2002.

[39] Hiratsuka T, Uezono M, Takakuda K, Kikuchi M, Oshima S, Sato T, et al. Enhanced bone formation onto the bone surface using a hydroxyapatite/collagen bone-like nanocomposite. ***J Biomed Mater Res B Appl Biomater.*** 108: 391-398, 2020.

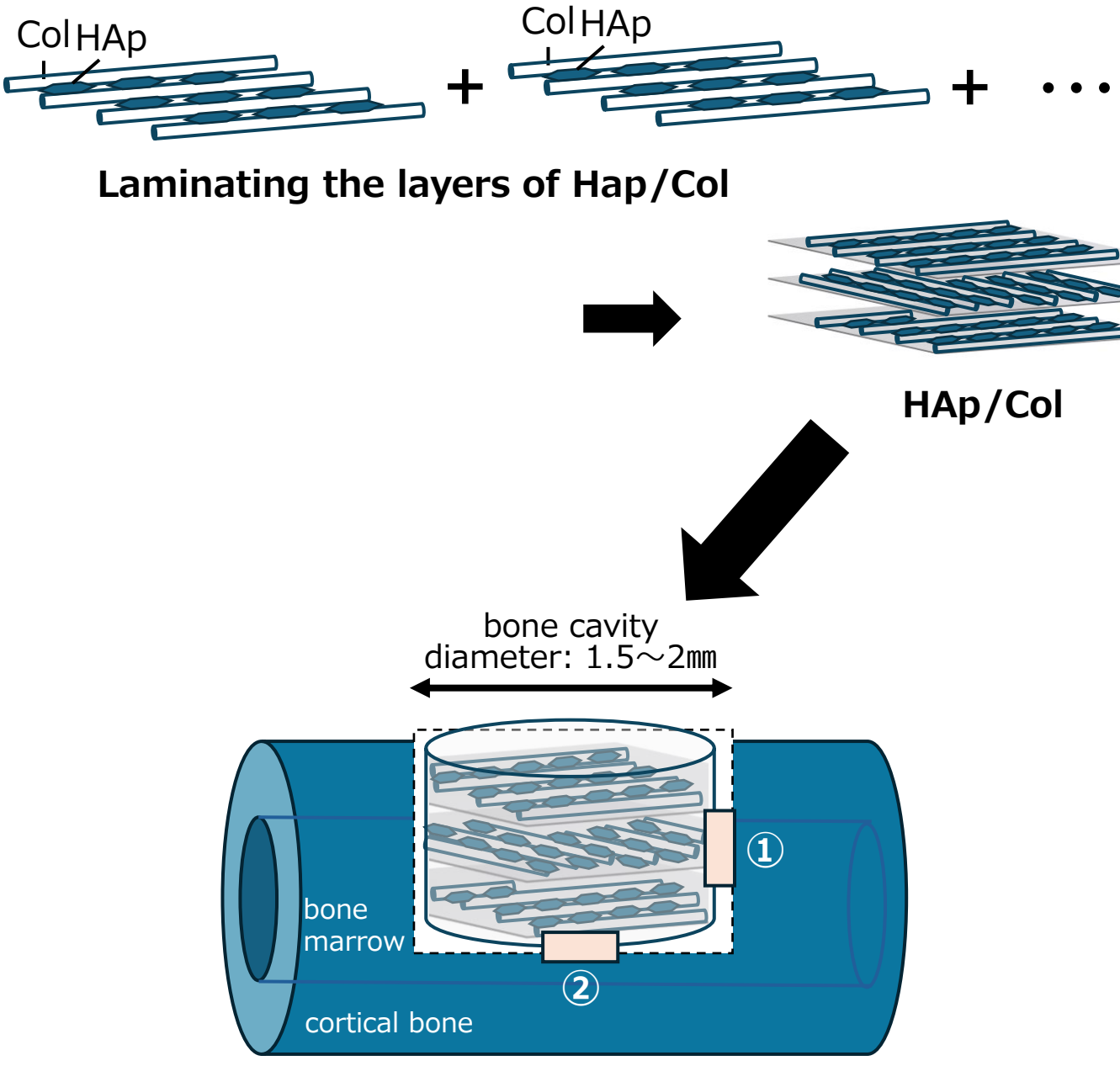

Regions of Interest
① : the region perpendicular to the collagen layers: lateral region
② : the region parallel to the collagen layers: bottom region

Figure 1

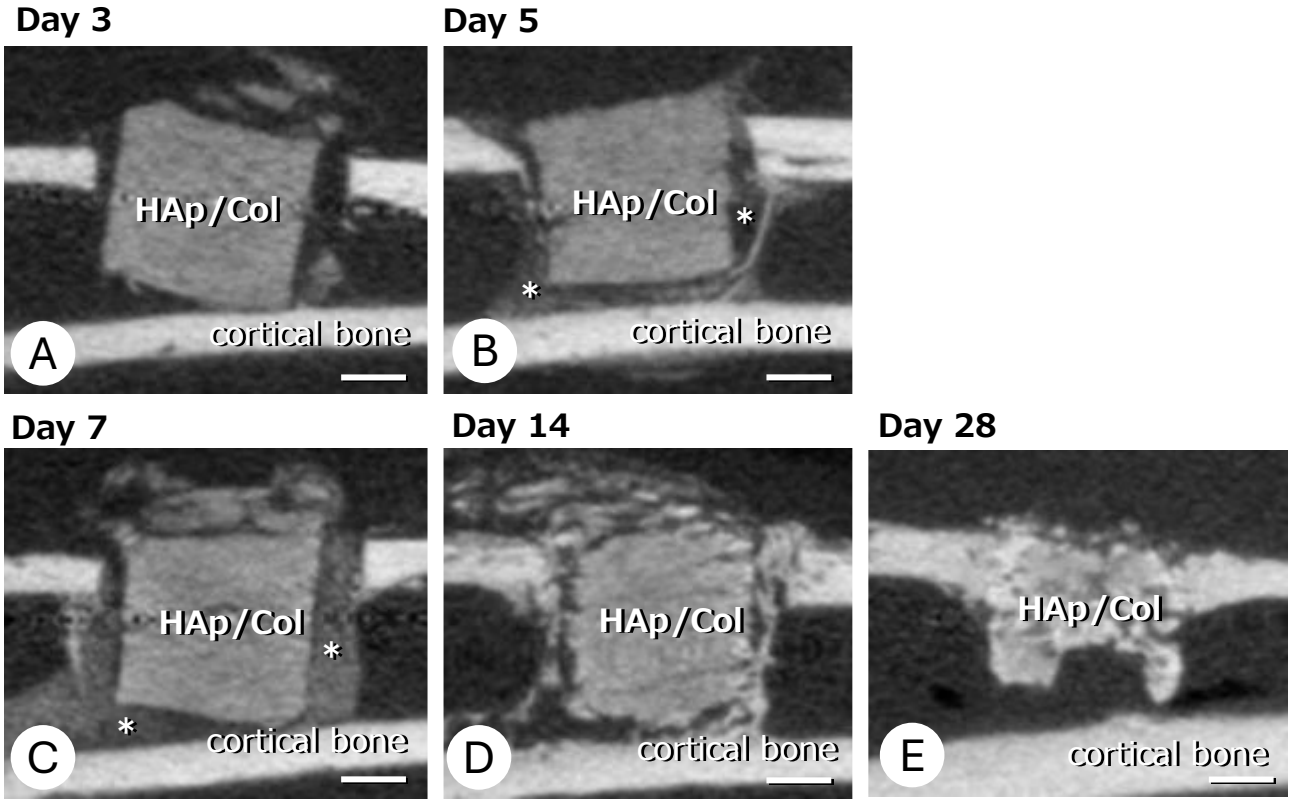
Day 3
HAp/Col
cortical bone
A
Day 5
HAp/Col
*
*
cortical bone
B
Day 7
HAp/Col
*
*
cortical bone
C
Day 14
HAp/Col
cortical bone
D
Day 28
HAp/Col
cortical bone
E

Figure 2

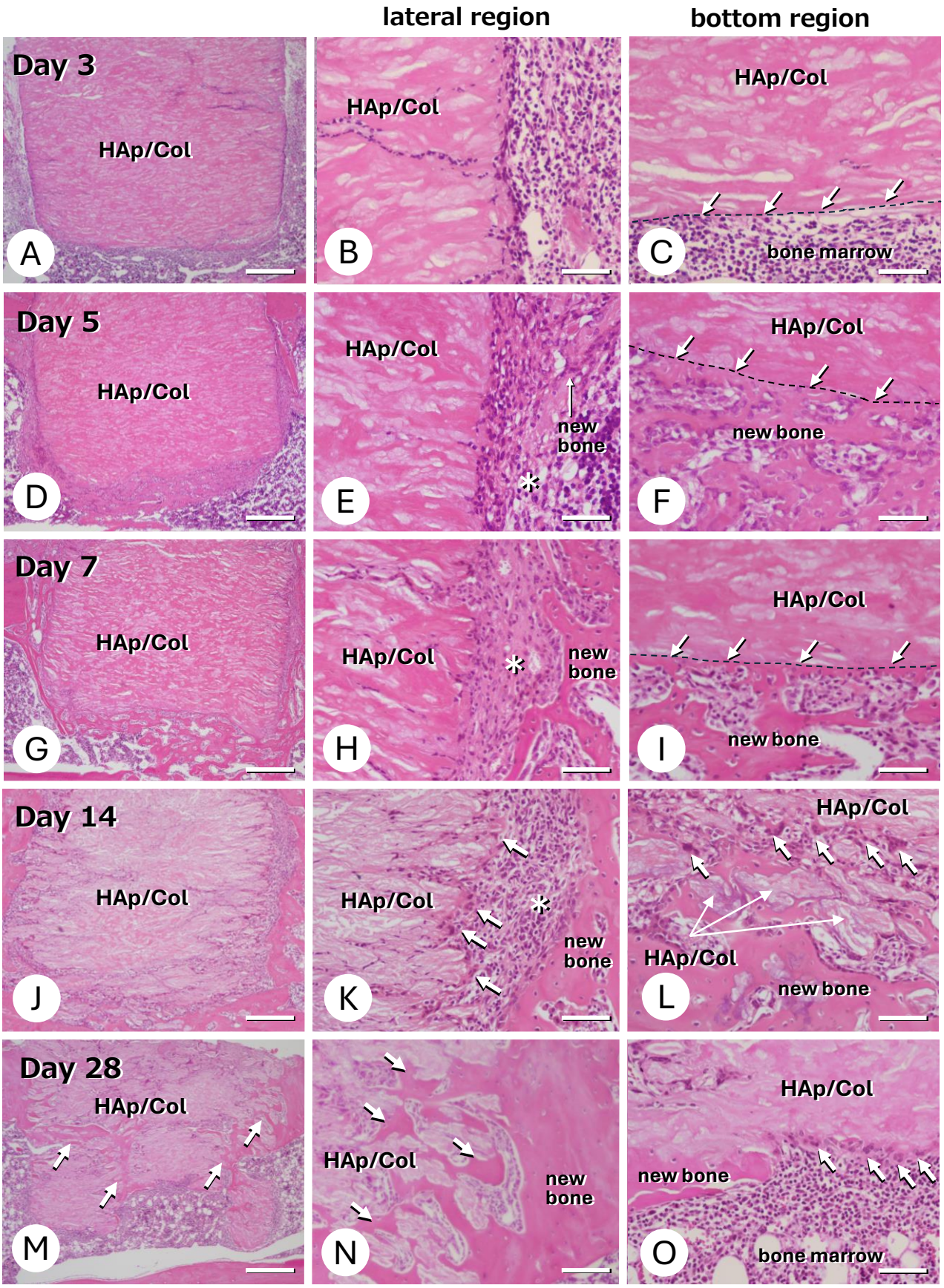
lateral region
bottom region
Day 3
HAp/Col
A
HAp/Col
B
HAp/Col
bone marrow
C
Day 5
HAp/Col
D
HAp/Col
new bone
*
E
HAp/Col
new bone
F
Day 7
HAp/Col
G
HAp/Col
*
new bone
H
HAp/Col
new bone
I
Day 14
HAp/Col
J
HAp/Col
*
new bone
K
HAp/Col
HAp/Col
new bone
L
Day 28
HAp/Col
M
HAp/Col
new bone
N
HAp/Col
new bone
bone marrow
O

Figure 3

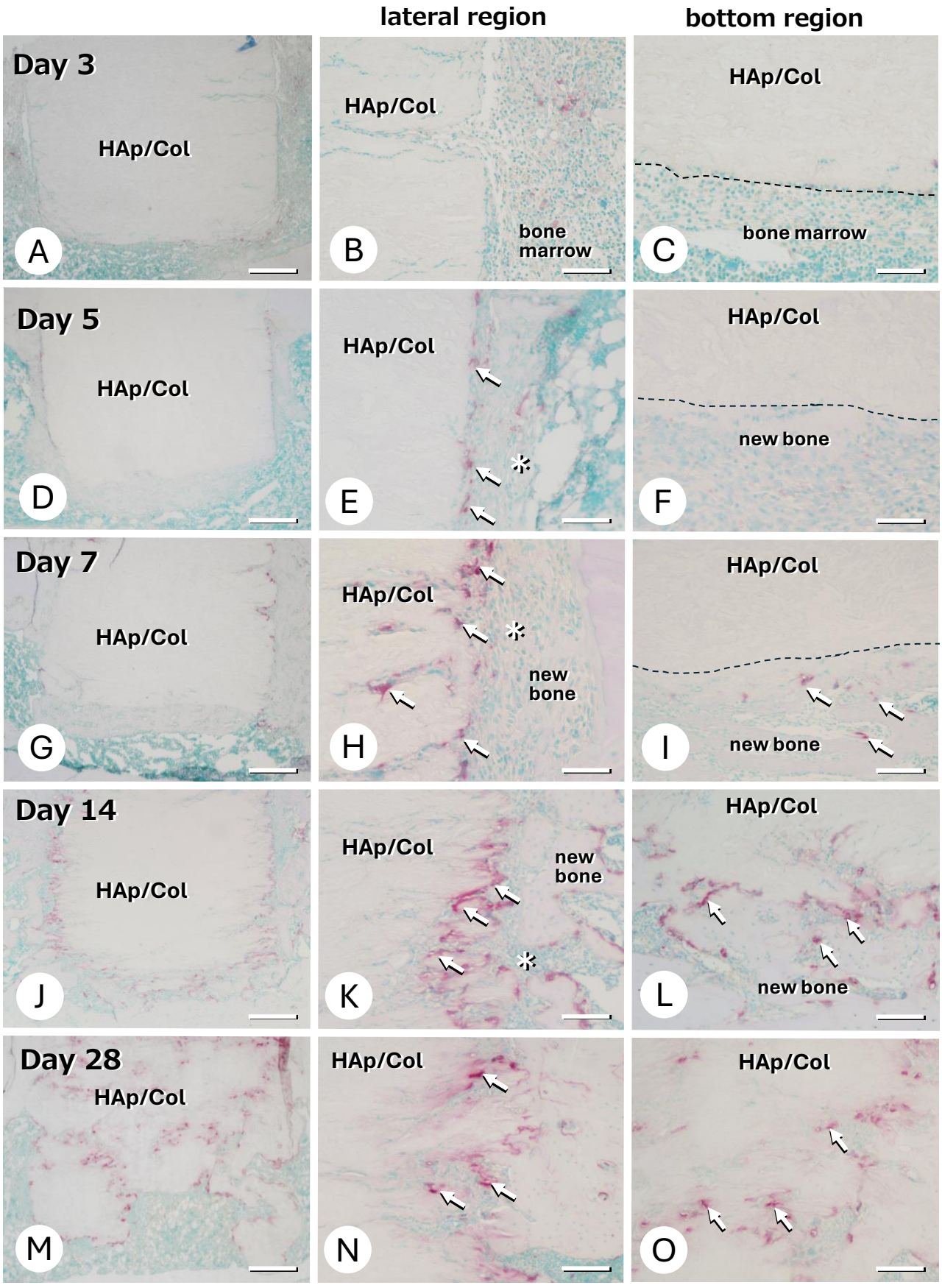
lateral region
bottom region
Day 3
HAp/Col
A
HAp/Col
bone marrow
B
HAp/Col
bone marrow
C
Day 5
HAp/Col
D
HAp/Col
E
HAp/Col
new bone
F
Day 7
HAp/Col
G
HAp/Col
new bone
H
HAp/Col
new bone
I
Day 14
HAp/Col
J
HAp/Col
new bone
K
HAp/Col
new bone
L
Day 28
HAp/Col
M
HAp/Col
N
HAp/Col
O

Figure 4

The numbers of TRAP-positive osteoclasts on the HAp/Col and newly-formed bone in ROIs

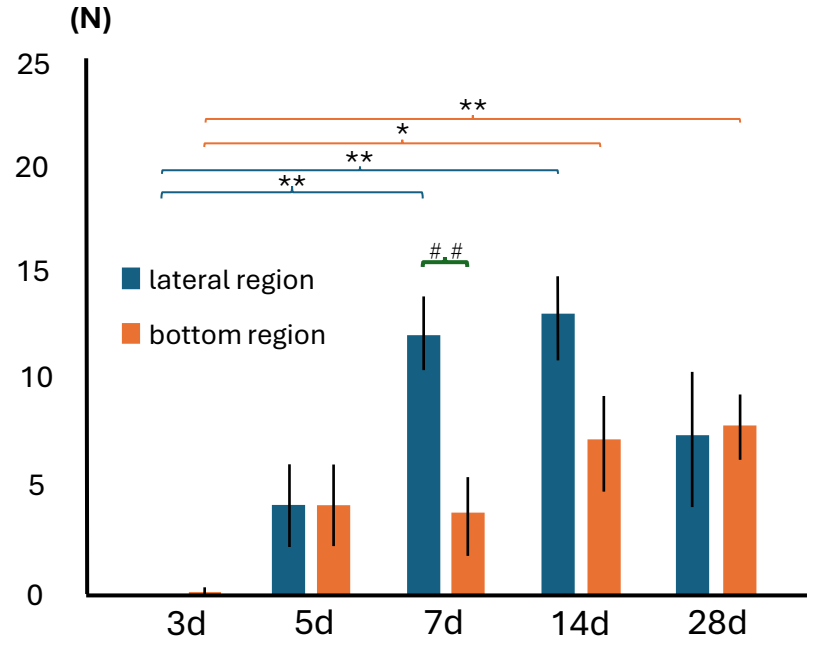

**: $p<0.01$
*: $p<0.05$
##: $p<0.01$

A

The total numbers of TRAP-positive osteoclasts in ROIs

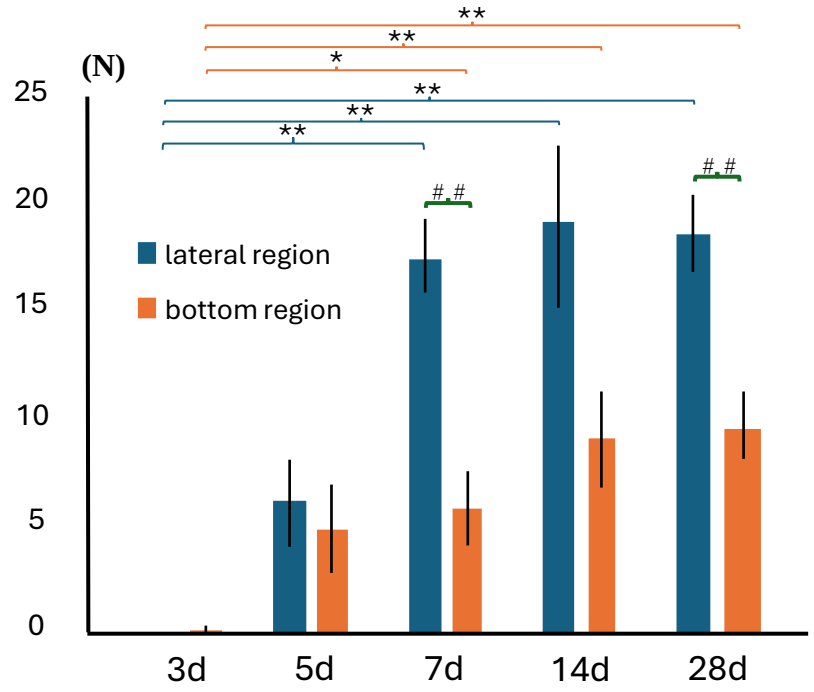

**: $p<0.01$
*: $p<0.05$
##: $p<0.01$

B

Figure 5

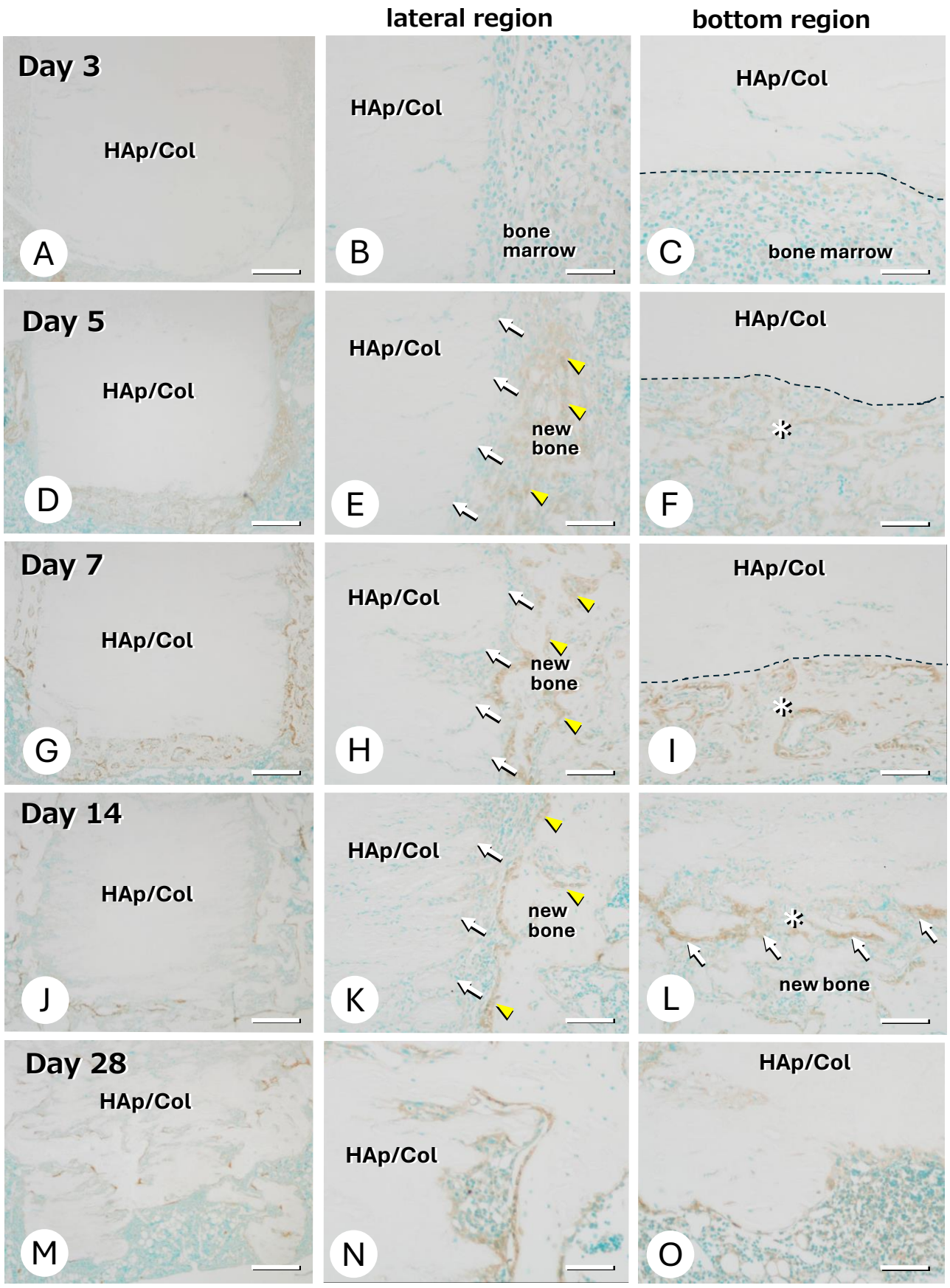
lateral region
bottom region
Day 3
HAp/Col
A
HAp/Col
bone
marrow
B
HAp/Col
bone marrow
C
Day 5
HAp/Col
D
HAp/Col
new
bone
E
HAp/Col
F
Day 7
HAp/Col
G
HAp/Col
new
bone
H
HAp/Col
I
Day 14
HAp/Col
J
HAp/Col
new
bone
K
new bone
L
Day 28
HAp/Col
M
HAp/Col
N
HAp/Col
O

Figure 6

The numbers of PHOSPHO1-positive osteoblasts on the HAp/Col and newly-formed bone in ROIs

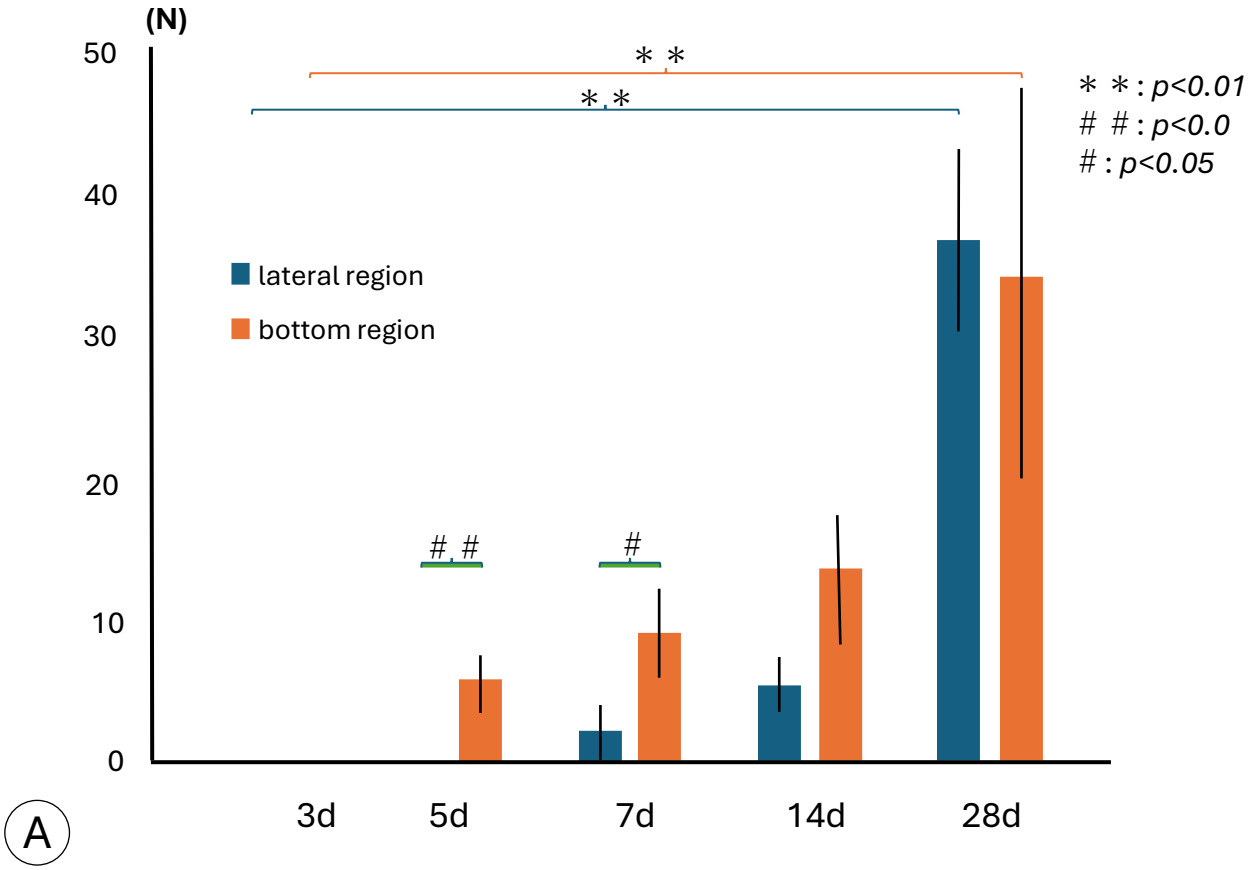

Figure 7

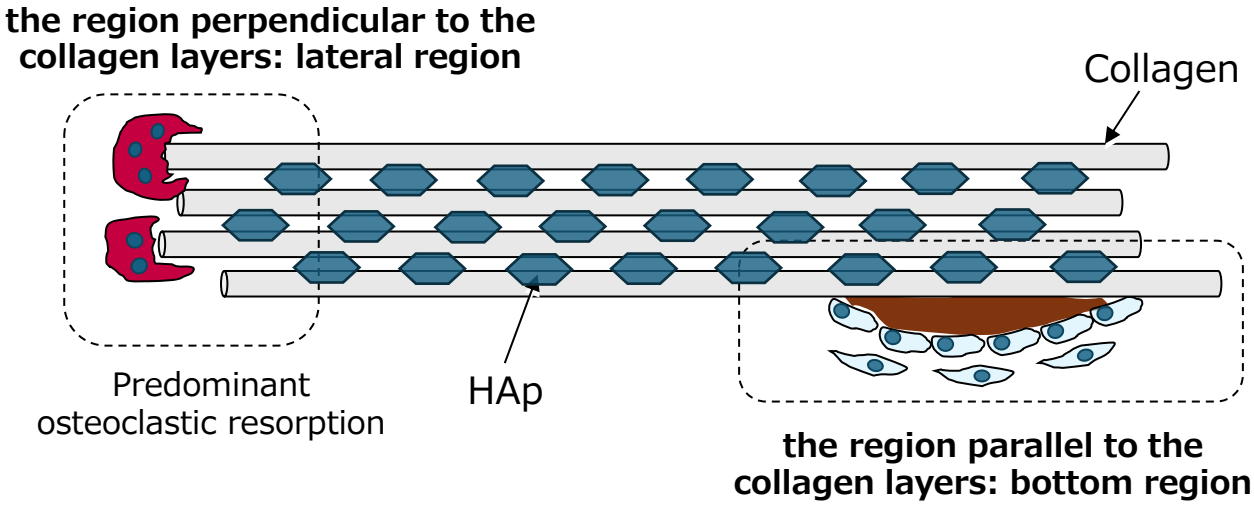
the region perpendicular to the collagen layers: lateral region
Collagen
Predominant osteoclastic resorption
HAp
the region parallel to the collagen layers: bottom region

Figure 8

Figure legends

Figure 1

Schematic design of HAp/Col embedding into rat tibiae

A cylinder of HAp/Col with a diameter of 1.5 mm and a height of 1.5 mm was implanted into a 1.5–2.0 mm diameter bone defect in the arterial center of the right tibia of 10-week-old male Wistar rat. Two 300 × 900 μm rectangular regions of interest (ROIs) were set up located in the center of the lateral (perpendicular to the collagen layers) and bottom (parallel to the collagen layers) regions of the HAp/Col cylinder.

Figure 2

Micro-CT images of the HAP/Col cylinder taken 3–28 days after grafting into the bone cavities

The micro-CT images reveal a semi-transparent tissue around the HAp/Col cylinders on days 5 and 7 that was not present 3 days after grafting **(**asterisks, **A-C)**. By day 14, trabecular bone is apparent around the cylinder, while the surface appears roughened **(D)**. On day 28, the HAp/Col cylinder and the adjacent cortical bone are well-integrated with each other, and the bottom regions of the cylinder have been eroded **(E)**. The scale bar represent 500 μm.

Figure 3

H-E staining on HAp/Col cylinder graft

Panels **A–C**, **D–F**, **G–I**, **J–L**, and **M–O** were obtained 3, 5, 7, 14, and 28 days after the HAp/Col grafting, respectively. Panels **A**, **D**, **G**, **J**, and **M** are low-magnification images of the HAP/Col cylinder. Panels **B**, **E**, **H**, **K**, and **N** and **C**, **F**, **I**, **L**, and **O** are histological images from the lateral and bottom regions, respectively. On day 3, the surface of the grafted HAp/Col cylinders look smooth, being surrounded by bone marrow tissue **(A–C)**. The dotted line indicates the boundary between the HAp/Col graft and the bone marrow **(C)**. On days 5 and 7, trabecular new bone is seen around the HAp/Col cylinder **(D, G)**. Trabecular new bones are continuous with the bottom surface of the cylinder **(F, I)**, whereas the new bones are discontinuous from the cylinder's lateral surface, with intervening stromal tissues (asterisks, **E, H)**. The dotted line indicates the boundary between the HAp/Col graft and the newly formed bone **(F, I)**. On day 14, in the lateral region, no continuity between the newly formed bone and the HAp/Col cylinder is seen yet due to intervening stromal tissue **(**asterisks, **J, K)**. Numerous multinucleated cells are localized on the lateral surface of the HAp/Col cylinder **(**arrows, **K)**, while the

bottom region has been fragmented into islands, with newly formed bone filling the spaces between them **(L)**. Note the multinucleated giant cells at the boundary between the HAp/Col graft and the new bone **(**arrows, **L)**. By day 28, the HAp/Col cylinder had collapsed, and newly formed bone had penetrated its interior in both the lateral and bottom regions **(M–O)**. The scale bars in **A, D, G, J,** and **M** represent 300 μm, while those in **B, C, E, F, H, I, K, L, N,** and **O** represent 100 μm.

Figure 4

Distribution of TRAP-positive osteoclasts

Panels **A–C**, **D–F**, **G–I**, **J–L**, and **M–O** were obtained 3, 5, 7, 14, and 28 days after the HAp/Col grafting respectively. Panels **A**, **D**, **G**, **J**, and **M** are low-magnification images of the HAP/Col cylinders. Panels **B**, **E**, **H**, **K**, and **N** and **C**, **F**, **I**, **L**, and **O** are histological images from the lateral and bottom regions, respectively. On day 3, TRAP-positive osteoclasts are nearly absent around the HAp/Col cylinder **(A–C)**. The dotted line indicates the boundary between the HAp/Col graft and the bone marrow **(C)**. On day 5, several TRAP-positive osteoclasts (red color, arrows) are localized along the lateral surface of the cylinder but not the bottom surface **(D–F)**. The dotted line indicates the boundary between the HAp/Col and newly formed bone **(F)**. The asterisks indicates stromal tissues **(E, H, K)**. By days 7 and 14, many TRAP-positive osteoclasts (arrows) have accumulated on the bumpy lateral surface of the HAp/Col cylinder **(G, H, J, K)**, allowing them to invade the cylinder's interior **(H, K)**. In contrast, in the bottom region, TRAP-positive osteoclasts (arrows) are seen in small numbers on day 7, but many were present on day 14 **(I, L)**. The dotted line indicates the boundary between the HAp/Col graft and the newly formed bone **(I)**. By day 28, TRAP-positive osteoclasts had completely invaded the HAp/Col cylinder **(M–O)**. The scale bars in **A, D, G, J,** and **M** represent 300 μm, while those in **B, C, E, F, H, I, K, L, N,** and **O** represent 100 μm.

Figure 5

Statistical analysis of the distribution of TRAP-positive osteoclasts

Panel **A** shows the number of TRAP-positive osteoclasts attached to the HAp/Col cylinder's surfaces, while panel **B** represents the total number of osteoclasts in the ROIs. The data are shown as the mean ± SE. Significant differences ($P < 0.05$) among means are represented using symbols: *, $P < 0.01$ and **, $P < 0.001$, for Dunnett's test results, and $^{\#\#}$, $P < 0.001$ for student's *t*-test results.

Figure 6

Distribution of PHOSPHO1-positive osteoblasts

Panels **A–C**, **D–F**, **G–I**, **J–L**, and **M–O** were obtained from 3, 5, 7, 14, and 28 days after the HAp/Col grafting, respectively. Panels **A**, **D**, **G**, **J**, and **M** are low-magnification images of the HAP/Col cylinders. Panels **B**, **E**, **H**, **K**, and **N** and **C**, **F**, **I**, **L**, and **O** are histological images from the lateral and bottom regions, respectively. On day 3, PHOSPHO1-positive osteoblasts are nearly absent from the surface of the HAp/Col cylinder **(A–C)**. The dotted line indicates the boundary between the HAp/Col graft and the bone marrow **(C)**. On days 5−7, PHOSPHO1-positive osteoblasts (brown color) can be seen in the new bone tissue around the HAp/Col cylinder **(D, G)**. In the lateral regions of the HAp/Col cylinder, PHOSPHO1-positive osteoblasts (arrowheads) were seen in the new bone tissue at a distance from the lateral cylinder surface but not on the surface itself **(E, H**; note that no PHOSPHO1-positive cells are visible on the HAP/Col cylinder surface, as indicated by arrows**)**. However, PHOSPHO1-positive osteoblasts are located in the new bone tissue (asterisks) extending from the bottom surface of the cylinder **(F, I)**. The dotted line indicates the boundary between the HAp/Col graft and the newly formed bone **(F, I)**. On day 14, PHOSPHO1-positive osteoblasts (arrowheads) can be seen on the trabecular bone at a distance from the lateral surface (arrows) of the HAp/Col cylinder but are still absent on the surface **(K)**, whereas lines of PHOSPHO1-positive osteoblasts (arrows) were noted on the newly formed bone (asterisk) in the bottom region **(L)**. By day 28, rows of PHOSPHO1-positive osteoblasts are observed throughout the HAp/Col cylinder **(M–O)**. The scale bars in **A, D, G, J,** and **M** represent 300 μm, while those in **B, C, E, F, H, I, K, L, N,** and **O** represent 100 μm.

Figure 7

Statistical analysis of the distribution of PHOSPHO1-positive osteoblasts

Panel **A** shows the number of TRAP-positive osteoclasts attached to the HAp/Col cylinder's surface, while panel **B** represents the total number of osteoclasts in the ROIs. The data are shown as the mean ± SE. Significant differences ($P < 0.05$) among means are represented using symbols: *, $P < 0.01$ and **, $P < 0.001$, for Dunnett's test results, and $^{\#\#}$, $P < 0.01$ and $^{\#}$, $P < 0.05$ for student's *t*-test results.

Figure 8

A schematic illustrating the findings of our study

After embedding an HAp/Col graft with laminated plates of horizontally orientated collagen fibers into the cavity defect in the tibia of a rat, osteoclasts accumulate in the region where the collagen fiber ends are exposed, while osteoblasts tend to adhere and induce bone formation in the regions where the collagen fibers run parallel to the bone tissue surface.